Chapter 6

3-Hydroxyquinoxaline–2–carboxalidine–2–amino thiophenol complexes of manganese(II), cobalt(II), nickel(II), copper(II) and zinc(II)

Contents

6.1 INTRODUCTION

The interest in studying Schiff bases containing ONS donors arose from their significant antifungal, antibacterial, and anticancer activities [1, 2]. In addition, the presence of both a hard and a soft donor group in one ligand increases the coordination ability towards hard as well as soft acidic metals. The structural features of the ONS donor salicylidine Schiff base complexes were reviewed by Soliman and Linert [3]. Anaconda and coworkers have shown that the condensation of an aldehyde or a ketone with 2-aminobenzenethiol does not lead to isolation of the corresponding Schiff base, but to the isolation of benzothiazoline [4, 5]. Nevertheless, in solution, the benzothiazolidine may exist in equilibrium with its tautomeric Schiff base which could be stabilized as its metal complex and cannot be isolated free of its associated metal ion. Bouwman *et al*. [6] reported the coexistence of the Schiff base *N*-(2'-*tert*-butylbenzylidene)-2-aminothiophenol and the ring closed 2-(2-*tert*-butylthiophenyl)benzothiazolidine in solution. The structure of the compounds in equilibrium mixture is given in figure 6.1. The

presence of a metal ion can prevent the formation of benzothiazolidines and can act as a templating agent for the formation of the Schiff base [7].

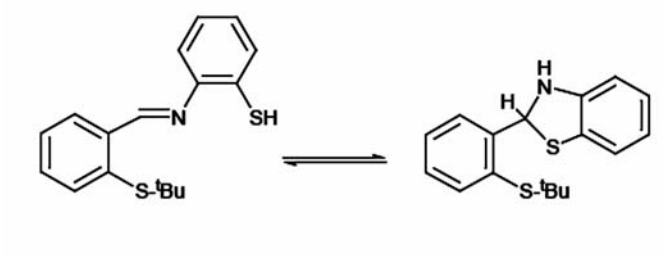

Figure 6.1: Schematic drawing of *N*-(2'-*tert*-butylbenzylidene)-2-aminothiophenol and 2-(2-*tert*-butylthiophenyl)benzothiazolidine in equilibrium

The Schiff base ligand generated by condensing 2-aminothiophenol with salicylaldehyde exhibits a remarkably diverse chemistry. Most importantly, the Schiff base, which is not the stable form of this noncoordinated molecule, undergoes ring closure to form benzothiazoline compounds [8-10]. Benzothiazoline compounds find application in medicine as as antiulcer drugs [11]. These compounds get rearranged to form the dianionic form of the Schiff base which can be stabilized by coordination to metal ion centers. There are many reports on the Schiff base complexes derived from 2-aminothiophenol with salicylaldehyde [9, 10, 12, 13]. But Schiff bases derived from 3-hydroxyquinoxaline-2-carboxaldehyde and 2-aminothiophenol are hithero unknown.

We have synthesized the benzothiazoline compound, 3-(2,3-dihydro-1,3-benzothiazol-2-yl)quinoxalin-2(1*H*)-one, which is abbreviated as btq. The formation of btq is given in scheme 6.1. In solution btq gets rearranged to form the corresponding Schiff base in presence of metal ion as given in scheme 6.2. In such condition, the Schiff base exhibits tautomerism and its keto/enol form is able to complex with metal ions. We have synthesised the Mn(II), Co(II), Ni(II), Cu(II) and Zn(II) complexes of this new Schiff base, 3–hydroxyquinoxaline–2–carboxalidine–2–aminothiophenol (hatp) and the complexes have been characterized by various physicochemical and spectroscopic techniques. In this chapter, the results of our studies on these complexes are presented.

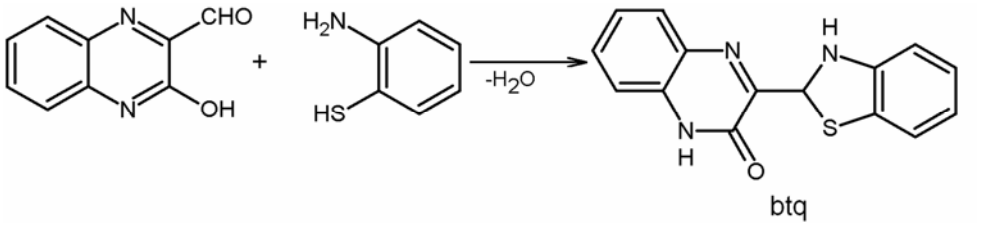

Scheme 6.1: ***The formation of btq by ring closure***

6.2 EXPERIMENTAL

6.2.1 Materials and methods

The procedures for the preparation of 3-hydroxyquinoxaline-2-carboxaldehyde and the techniques employed for the characterization of btq and metal complexes are given in chapter II.

6.2.2 Preparation of 3-(2,3-Dihydro-1,3-benzothiazol-2-yl)quinoxalin-2(1*H*)-one

The compound, 3-(2,3-dihydro-1,3-benzothiazol-2-yl)quinoxalin-2(1*H*)-one, was prepared by taking an aqueous solution of 3–hydroxyquinoxaline –2–carboxaldehyde (1.742 g, 10 mmol, in 500 mL distilled water) which is acidified using 3–4 drops of con. HCl. To this solution was added a solution of 2–aminothiophenol (1.07 mL, 10 mmol) in methanol (20 mL) dropwise. The solution was stirred for 6 hours. The precipitated Schiff base was filtered, washed with water and dried over anhydrous calcium chloride. The crude product was recrystallised from absolute ethanol. Yield: 2.3 g (81.73 %)

6.2.3 Preparation of Complexes

The complexes of manganese(II), cobalt(II), nickel(II), copper(II) and zinc(II) were prepared by the following general procedure:

The compound btq (0.29 g, 1 mmol) dissolved in methanol (30 mL) was mixed with the solution of the metal salt (1 mmol: 0.245 g of $Mn(OAc)_2.4H_2O$, 0.249 g of $Co(OAc)_2.4H_2O$, 0.2488 g of $Ni(OAc)_2.4H_2O$, 0.1705 g of $CuCl_2.2H_2O$ or 0.2195 g of $Zn(OAc)_2.2H_2O$) in methanol (10 mL) and was stirred for 3 hours at room temperature (27±2 ºC). The precipitate formed was filtered off, washed with cold methanol, and dried in vacuum over anhydrous calcium chloride.

Our attempts to synthesize iron(III) complex of the Schiff base were not successful. In this case, we could get only the starting compound.

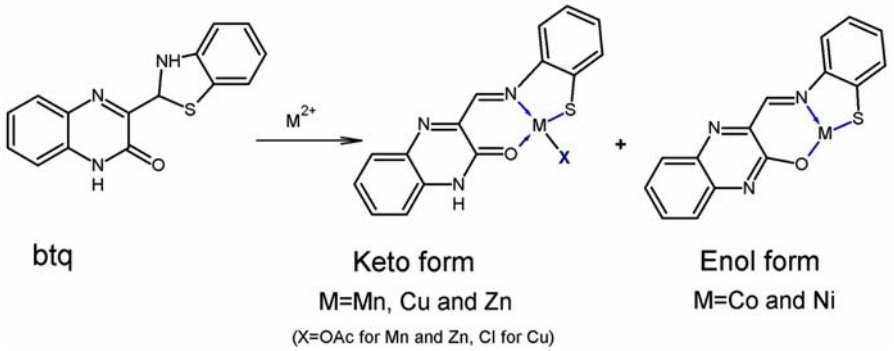

Scheme 6.2: ***Formation of metal complexes of btq***

6.3 RESULTS AND DISCUSSION

Spectral data of the yellow compound isolated from the reaction of 3-hydroxyquinoxaline-2-carboxaldehyde and 2–aminothiophenol indicate that the compound does not have the expected open chain imine, but has a benzothiazoline structure as depicted in scheme 6.1. Similar reactions leading to the formation of benzothiazolines from 2–mercaptoanilines have been reported [7-9, 11, 12]. The product 3–(2,3–dihydro–1,3–benzothiazol–2–yl)quinoxalin-2(1*H*)–one (abbreviated as btq) was characterized by elemental analysis, IR and ^{1}H NMR spectra. The Mn(II), Co(II), Ni(II), Cu(II) and Zn(II) complexes were prepared by the stoichiometric reaction of the metal chloride/acetate with the compound, btq. The complexation

reaction proceeds with the rearrangement of btq to the corresponding Schiff base, hatp.

The colour, yield and elemental analyses data of btq and the complexes of its rearranged form, hatp, are given in Table 6.1. The molar conductivity values (table 6.2) in 10^{-3} M DMF solutions suggest non-electrolytic nature of the complexes [14]. The analytical data reveal the metal ligand ratio as 1:1 for all the complexes.

Table 6.1: ***Analytical data of btq and complexes of hatp***

Compound	Colour	Yield (%)	Analytical data. Found (calculated)%					
			C	H	N	S	M	Cl
btq	Yelow	80	64.15 (64.04)	4.25 (3.94)	14.63 (14.94)	11.44 (11.40)	-	-
[Mn(hatp)(OAc)$(H_2O)_2$]	Red	56	48.38 (47.45)	3.85 (3.98)	9.95 (9.76)	7.50 (7.45)	12.45 (12.77)	-
[Co(hatp)$(H_2O)_3$]	Brown	75	43.68 (43.91)	3.70 (4.18)	10.33 (10.24)	8.07 (7.81)	14.79 (14.36)	-
[Ni(hatp)$(H_2O)_3$]	Red	63	45.37 (45.95)	3.28 (3.86)	10.60 (10.72)	8.09 (8.18)	15.31 (14.97)	-
[Cu(hatp)Cl]	Violet	70	47.38 (47.50)	2.40 (2.66)	11.12 (11.08)	8.42 (8.45)	16.41 (16.75)	8.92 (9.35)
[Zn(hatp)(OAc)]	Brown	78	50.17 (50.44)	3.28 (3.24)	10.60 (10.38)	8.09 (7.92)	16.31 (16.16)	-

Table 6.2: ***Conductivity and magnetic moment data of complexes***

Compound	$\lambda_m^{\#}$	μ_{eff} (B.M)
[Mn(hatp)(OAc)$(H_2O)_2$]	20	5.80
[Co(hatp)$(H_2O)_3$]	11	5.18
[Ni(hatp)$(H_2O)_3$]	16	3.27
[Cu(hatp)Cl]	14	1.95
[Zn(hatp)(OAc)]	12	-

$^{\#}$ Molar conductivity (in Mho cm^2 mol^{-1}), 10^{-3} Molar solution in DMF

6.3.1 ^{1}H NMR spectra of btq and [Zn(hatp)(OAc)]

The ^{1}H NMR spectra of the compound btq and that of [Zn(hatp)(OAc)] complex were recorded in d_6-dimethylsulphoxide solution using TMS as the internal standard. The chemical shifts of different protons of compound btq and of the zinc(II) complex are listed in table 6.3. Proton NMR spectra of btq and the zinc(II) complex are given in figures 6.2 and 6.3. The compound, btq, exhibits a doublet at 7.16 ppm due to thiazolidine CH (*J*=5Hz) [6] and a multiplet at 7.4–8.3 ppm due to the two NH protons and 8 aromatic protons [15]. In the NMR spectrum of the diamagnetic zinc(II) complex, the azomethine proton appears at 8.93 ppm as a singlet [16] and the three acetate protons appear as a singlet at 1.23 ppm. The aromatic protons are observed in the region 7.0–7.9 ppm as a multiplet. Thus the spectrum of the zinc(II) complex is quite different from that of the compound, btq and the spectral data clearly reveal that the ring opening of btq occurs in presence of metal ion.

Table 6.3: ***^{1}H NMR Spectroscopic data of btq and [Zn(hatp)(OAc)]***

Compound	Chemical shift, δ (ppm)	Assignment
btq	7.16	(d, 1H, CH benzothiazoline)
	7.44-8.30	(m, 9H, Ar H and benzothiazoline NH)
	12.00-13.00	(m, 1H, NH/OH quinoxaline)
[Zn(hatp)(OAc)]	1.23	(s, 3H, CH_3 acetate)
	7.00-7.90	(m, 8H, Ar. H)
	8.93	(s, 1H, CH azomethine)
	12.20	(br s, 1H, NH)

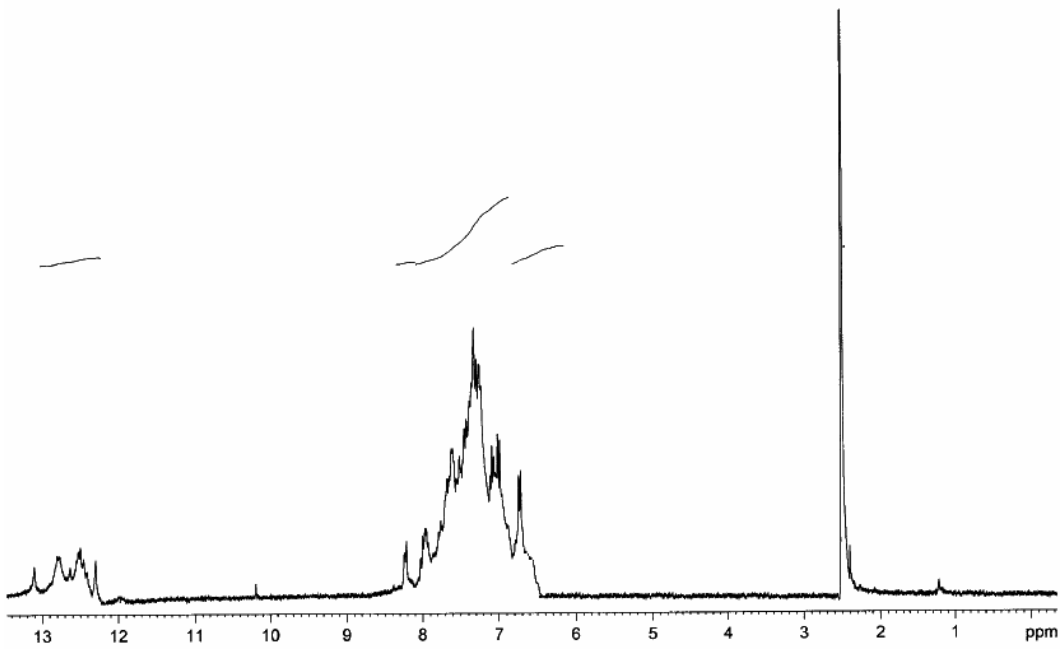

Figure 6.2: ***NMR spectrum of btq***

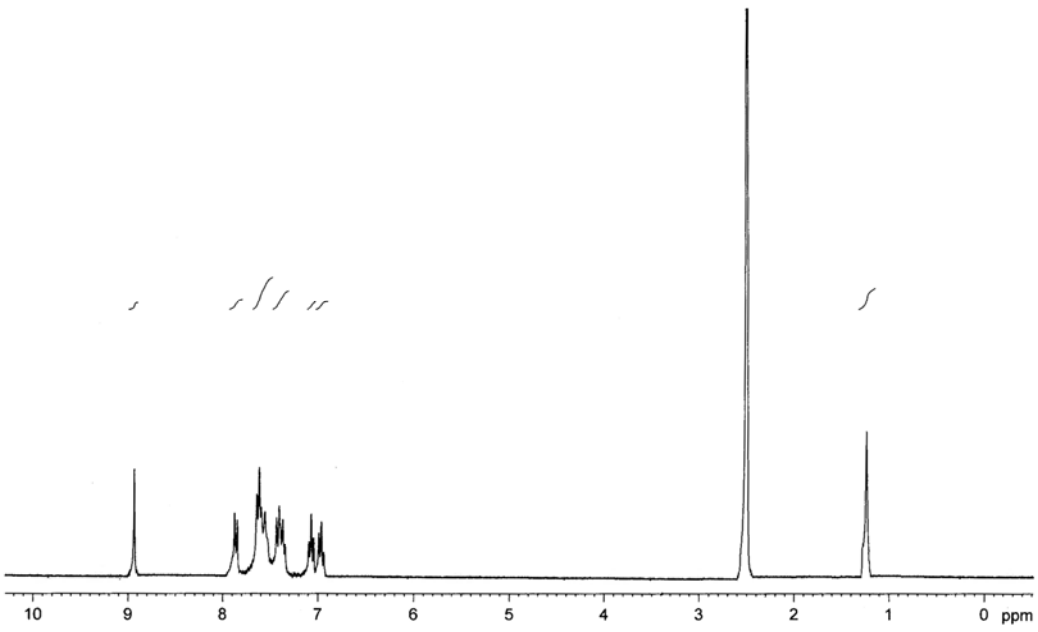

Figure 6.3: ***NMR spectrum of [Zn(hatp)(OAc)]***

6.3.2 Magnetic susceptibility measurements

The magnetic moment values of the complexes are presented in table 6.2. The μ_{eff} value of 5.80 B.M. for manganese(II) complex corresponds to the presence of five unpaired electrons and gives no specific information about its stereochemistry. The octahedral and tetrahedral cobalt(II) complexes differ in their magnetic properties. Because of the intrinsic orbital angular momentum in the octahedral ground state, there would be considerable orbital contribution, and effective magnetic moment values for such compounds at room temperature lie between 4.7 to 5.2 B.M. The complex, $[Co(hatp)(H_2O)_3]$, exhibits a magnetic moment of 5.18 B.M. which suggests an octahedral geometry for the complex [17, 18]. The nickel(II) complex is also octahedral, as it exhibits a μ_{eff} value of 3.27 B.M. [19]. The copper(II) complex has a magnetic moment of 1.95 BM, which indicate that the four coordinated complex is not tetrahedral.

6.3.3 Infrared spectra

The most important IR spectral bands of the btq and metal complexes of hatp are listed in Table 6.4. The benzothiazoline in presence of metal ion rearranges to form the Schiff base and the resulting Schiff base can act either in a monoanionic tridentate (keto form) or in a dianionic tridentate (enol form) manner as given in Scheme 6.2. The formation of benzothiazoline was confirmed by the absence of bands due to ν(SH) in the spectra of btq (Figure 6.4) [20]. Two absorption bands at 3375 and 3325 cm^{-1} due to ν(NH) of the amide tautomer and benzothiazoline ring respectively suggest the existence of btq in keto form in the solid state. In the case of tautomeric quinoxaline derivatives, particularly quinoxaline-2-ones, the IR stretching frequencies of the C=O and C=N (quinoxaline ring) vary from compounds to compounds [21]. It is not easy to assign a particular range for these two types of stretching frequencies. Mamedov *et al.* reported a series of quinoxaline-2-one compounds, which exhibit the C=O stretching in the region 1680–1665 cm^{-1} and quinoxaline C=N stretching in the

region 1600–1620 cm^{-1} [22-24]. In the IR spectrum of btq, the C=O and quinoxaline C=N stretching frequencies occur at 1665 and 1609 cm^{-1} respectively. The bands can be easily distinguished on the basis of their intensity, as the ν(C=O) will be more intense than ν(C=N).

The complexes exhibit a broad band in the range 3100–3500 cm^{-1}, due to the OH stretching of water molecules (Figures 6.5-6.9) [25]. The (N–H) stretching is also observed in the same region. However, we could not differentiate them due to the broadness of the peak. The Schiff base exists in the enol form in the cobalt(II) and nickel(II) complexes, which is evidenced by the disappearance of band due to (C=O) stretching. But it exists in the keto form in the manganese(II) copper(II) and zinc(II) complexes as there is a strong band around 1650 cm^{-1} for these complexes [26]. In these cases coordination of the ligand to metal ion is in a monoanionic tridentate manner. All the complexes exhibit the azomethine stretching in the region 1600–1640 cm^{-1} and the C–O (phenolic) stretching band is observed in the range of 1200–1300 cm^{-1} [27]. Conclusive evidence of the bonding is also shown by the appearance of new bands in the region 430-470 and 400-420 cm^{-1} in the spectra of the complexes due to (M–O) and (M–N) stretching vibrations [28-31].

Table 6.4: ***IR spectral data of btq and its complexes***

Assignments (in cm^{-1})	ν(OH) / ν(NH)	ν(C=O)	ν(C=N)#	ν(M–O)	ν(M–N)
btq	3375, 3325	1665	-	-	-
$[Mn(hatp)(OAc)(H_2O)_2]$	3300 b	1650	1637	431	419
$[Co(hatp)(H_2O)_3]\ H_2O$	3400 b	-	1629	465	422
$[Ni(hatp)(H_2O)_3]$	3400 b	-	1624	445	404
[Cu(hatp)Cl]	-	1676	1605	427	406
[Zn(hatp)(OAc)]	-	1657	1599	505	420

azomethine, b-broad

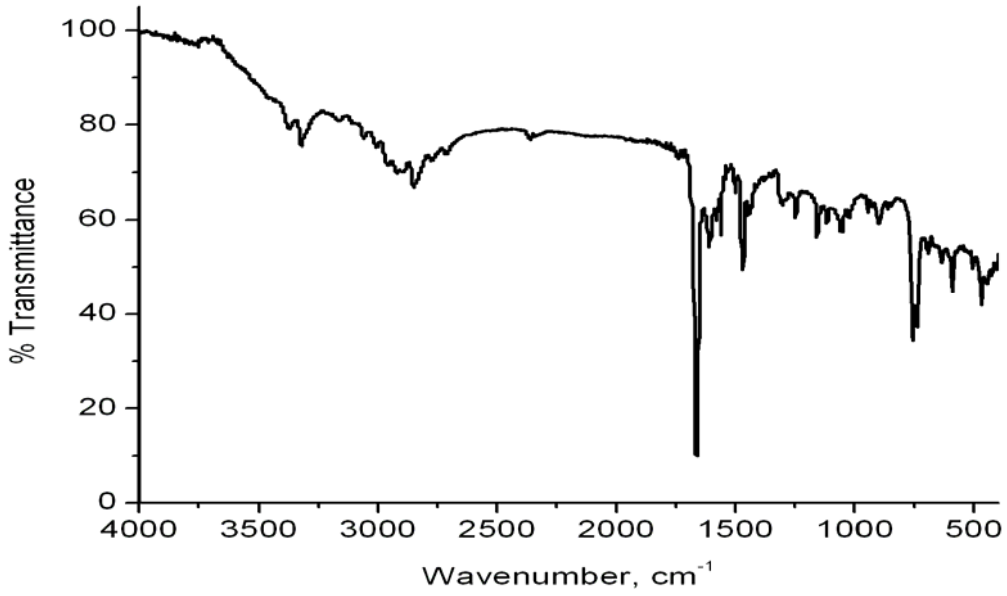

Figure 6.4: ***IR spectrum of btq***

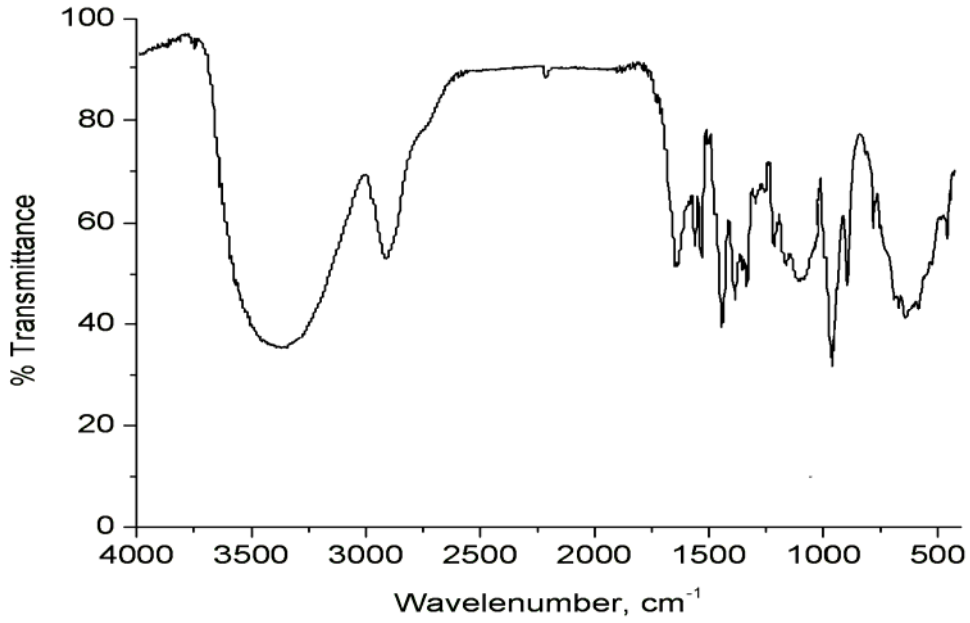

Figure 6.5: ***FTIR spectrum of [Mn(hatp)(OAc)(H$_2$O)$_2$]***

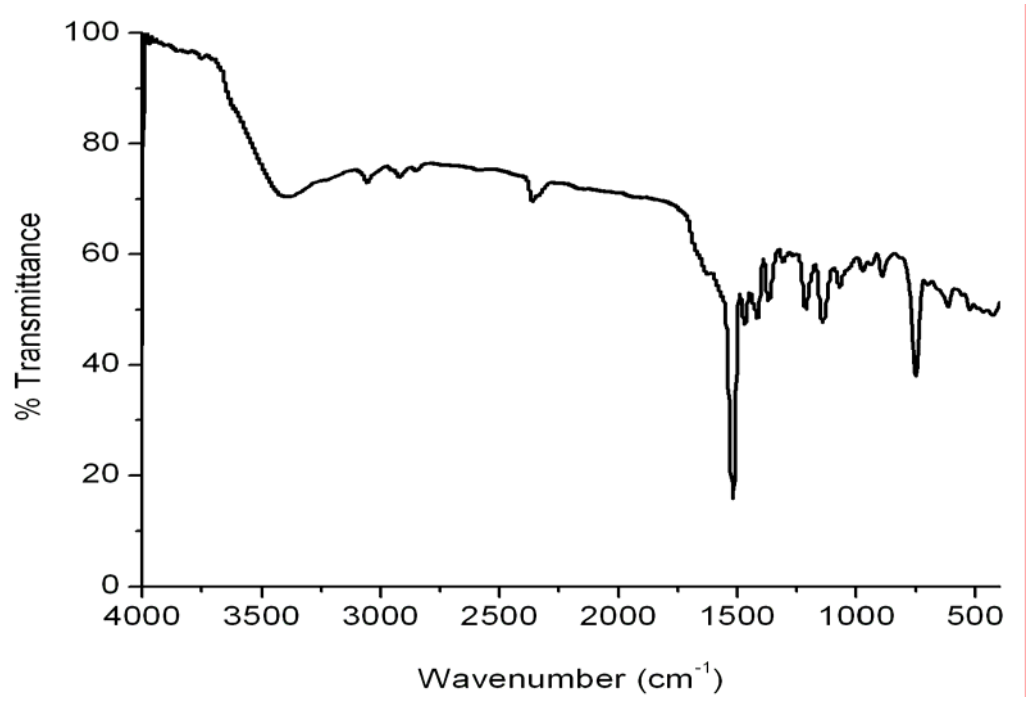

Figure 6.6: ***FTIR spectrum of [Co(hatp)(H$_2$O)$_3$] H$_2$O***

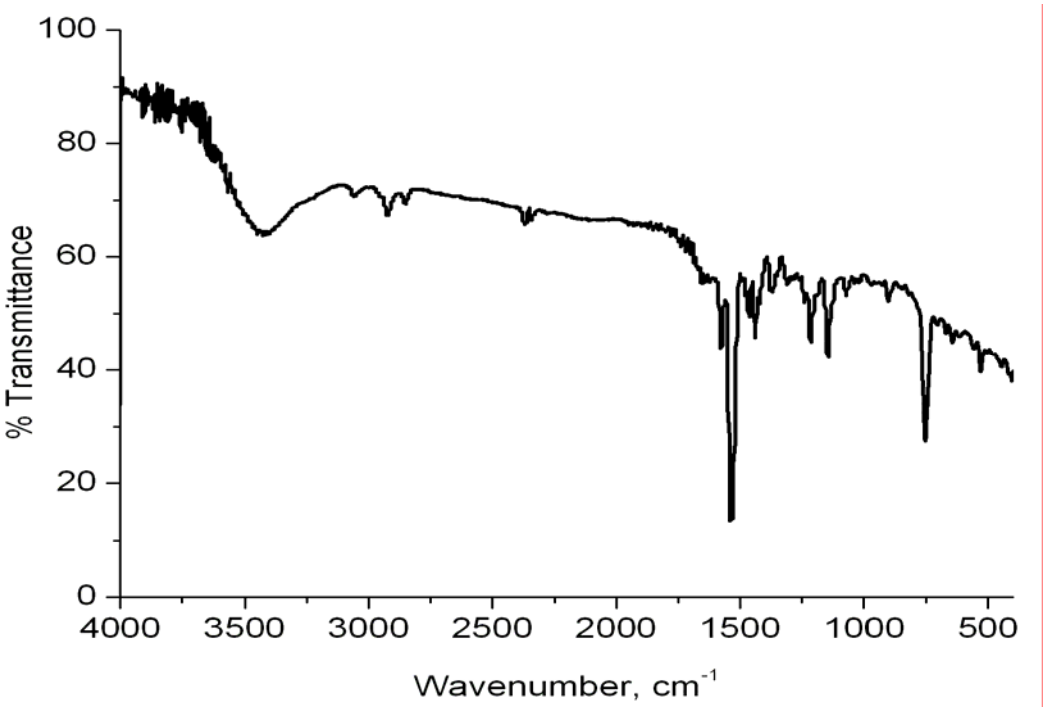

Figure 6.7: ***FTIR spectrum of [Ni(hatp)(H$_2$O)$_3$]***

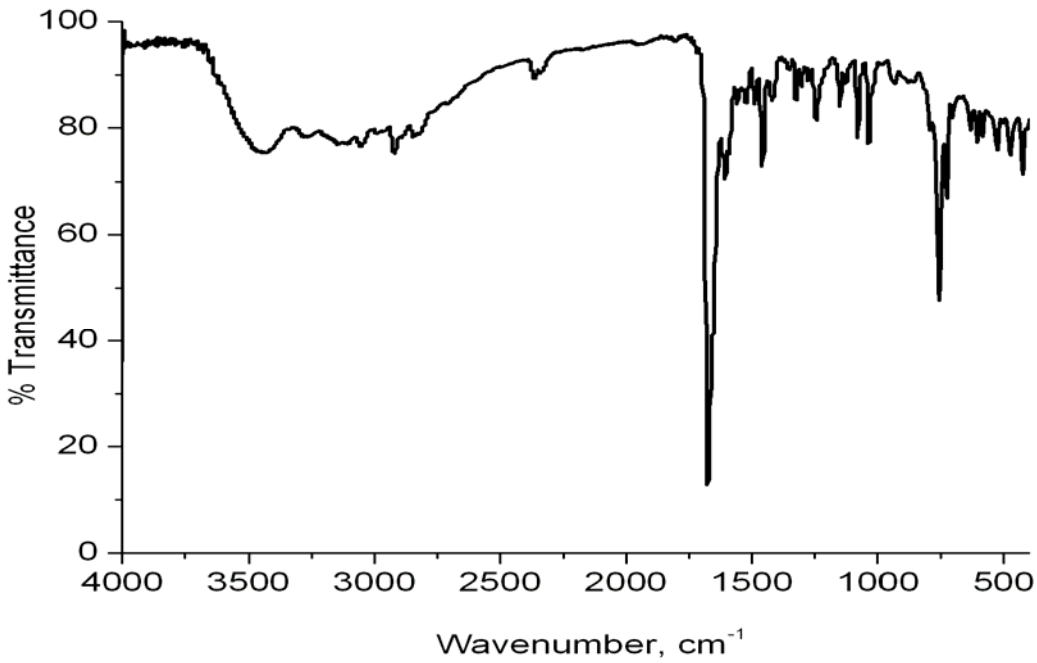

Figure 6.8: ***FTIR spectrum of [Cu(hatp)Cl]***

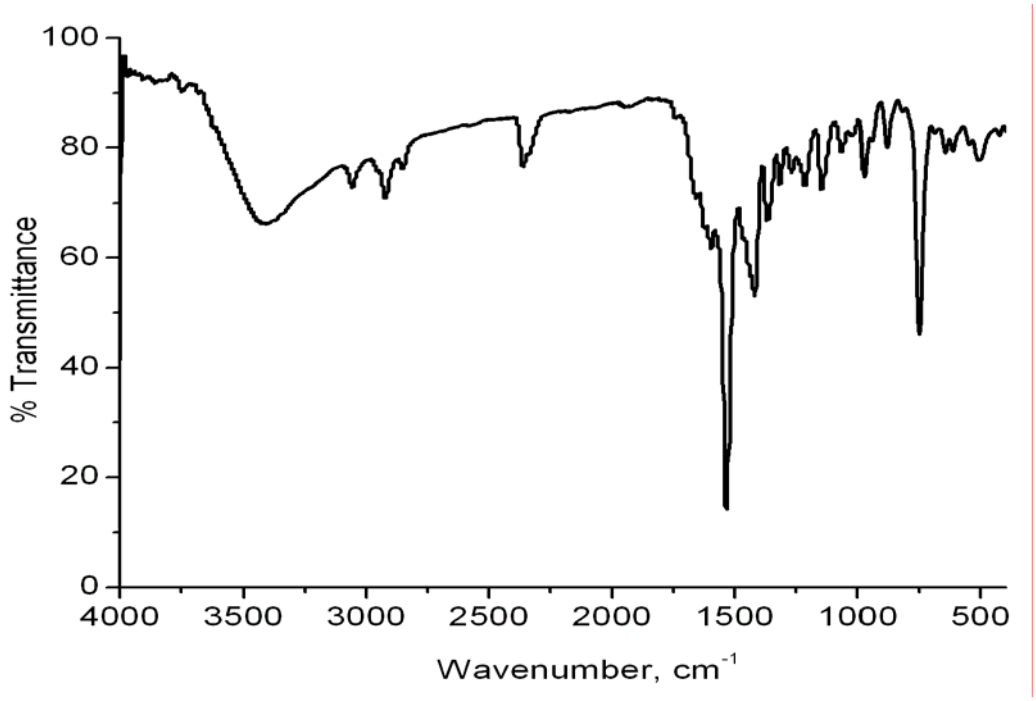

Figure 6.9: ***FTIR spectrum of [Zn(hatp)(OAc)]***

6.3.4 Electronic spectra

The UV–Vis spectra of the compound btq and the complexes of hatp are recorded in methanol in the wavelength range from 50000–10000 cm^{-1}. Electronic spectra of btq and the complexes of hatp are given in Figures 6.10-6.15. Spectral data are presented in Table 6.5. The bands at 37700 and 29000 cm^{-1} are attributed to quinoxaline π–π* and phenyl π–π* transitions respectively. The band at 25000 cm^{-1} is assigned to the n–π* transition of azomethine group and ring (C=N) groups.

The manganese(II) complex exhibits bands at 23500 and 21400 cm^{-1}, which can be assigned to $^6A_{1g}\rightarrow{}^4E_g(G)$ and $^6A_{1g}\rightarrow{}^4T_{2g}(G)$ transitions expected for the octahedral complexes of Mn(II) [32]. These transitions are forbidden and the intensity of the bands is found to be very low (log ε <1). The spectrum also shows bands at 24800 and 29600 cm^{-1} due to the metal to ligand to metal charge transfer transitions.

No d-d transitions were observed for the cobalt(II) complex. The complex exhibits a broad charge transfer band with a maximum at 19200 cm^{-1}, which might have obscured all the d-d transitions expected for an octahedral complex [33].

The three spin allowed electronic transitions are expected for octahedral nickel(II) complexes. The shoulder bands observed at 21370, 19530 and 11325 cm^{-1} can be assigned to the transition from $^3A_{2g}$ to $^3T_{2g}(F)$, $^3T_{1g}(F)$ and $^3T_{1g}(P)$ respectively. Furthermore intensities of these bands are very low as expected for the octahedral complexes [17, 32].

The copper(II) complex exhibits ligand to metal charge transfer transitions at 27800 and 24700 cm^{-1}. The d-d bands observed at 20200 and 17500 cm^{-1} are due to $^2B_{1g}\rightarrow{}^2E_g$ and $^2B_{1g}\rightarrow{}^2A_{1g}$ transitions expected for the square planar copper(II) complexes [34]. Two charge transfer transitions are observed at 29900 and 23500 cm^{-1} for the zinc(II) complex.

Table 6.5: ***UV-Vis spectral assignments of btq and complexes***

Compound	Absorption maxima (cm^{-1})	log ε (ε in L mol^{-1} cm^{-1})	Assignment
btq	37700	4.07	$\pi \rightarrow \pi^*$
	29000	3.62	$\pi \rightarrow \pi^*$
	25000	2.97	$n \rightarrow \pi^*$
$[Mn(hatp)(OAc)(H_2O)_2]$	37750	4.06	$\pi \rightarrow \pi^*$
	29600	2.54	CT
	24800	1.11	CT
	23500	0.90	$^6A_{1g} \rightarrow {}^4E_g(G)$
	21400	0.70	$^6A_{1g} \rightarrow {}^4T_{2g}(G)$
$[Co(hatp)(H_2O)_3]\ H_2O$	37000	3.89	$\pi \rightarrow \pi^*$
	32900	3.46	$\pi \rightarrow \pi^*$
	24600	2.63	$n \rightarrow \pi^*$
	19200	3.60	CT
$[Ni(hatp)(H_2O)_3]$	37700	3.95	$\pi \rightarrow \pi^*$
	29400	3.13	$n \rightarrow \pi^*$
	24700	3.69	CT
	23400	3.66	CT
	21400	2.18	$^3A_{2g} \rightarrow {}^3T_{2g}$
	19500	1.14	$^3A_{2g} \rightarrow {}^3T_{1g}$
	11300	1.17	$^3A_{2g} \rightarrow {}^3T_{1g}(P)$
[Cu(hatp)Cl]	37700	3.96	$\pi \rightarrow \pi^*$
	27800	3.54	CT
	24700	3.32	CT
	20200	2.95	$^2B_{1g} \rightarrow {}^2E_g$
	17500	2.85	$^2B_{1g} \rightarrow {}^2A_{1g}$
[Zn(hatp)(OAc)]	37750	3.92	$\pi \rightarrow \pi^*$
	29900	3.46	CT
	23500	3.30	CT

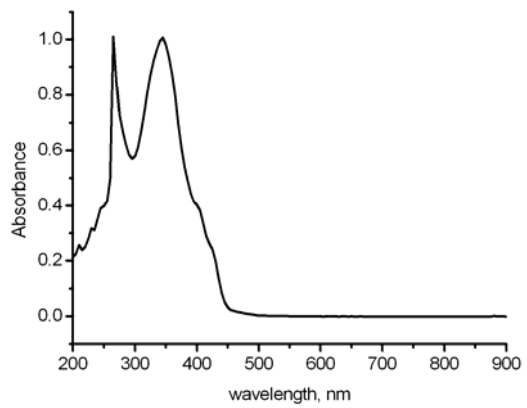

Figure 6.10: ***The UV-Vis spectrum of btq***

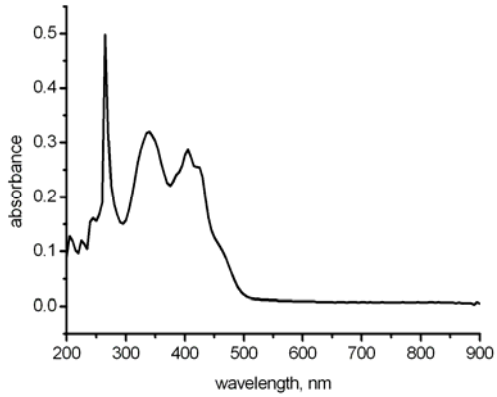

Figure 6.11: ***The UV-Vis spectrum of [Mn(hatp)(OAc)(H$_2$O)$_2$]***

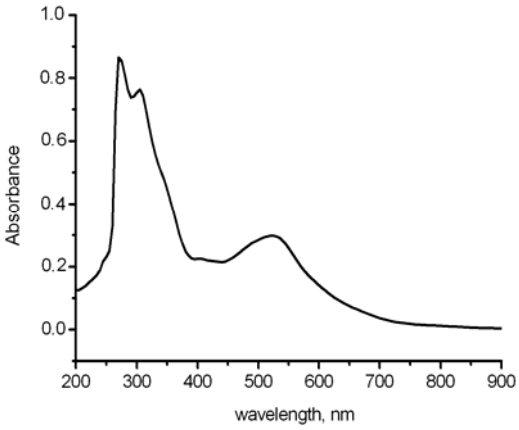

Figure 6.12: ***The UV-Vis spectrum of [Co(hatp)(H$_2$O)$_3$] H$_2$O***

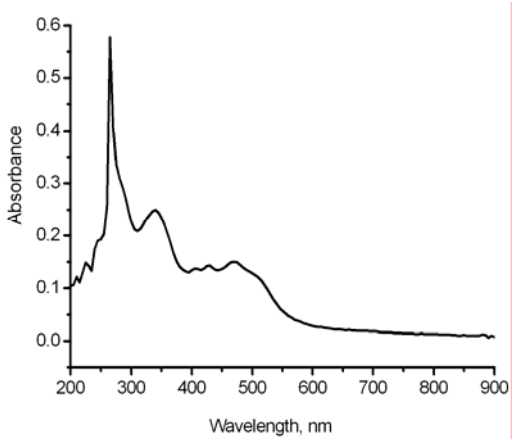

Figure 6.13: ***The UV-Vis spectrum of [Ni(hatp)(H$_2$O)$_3$]***

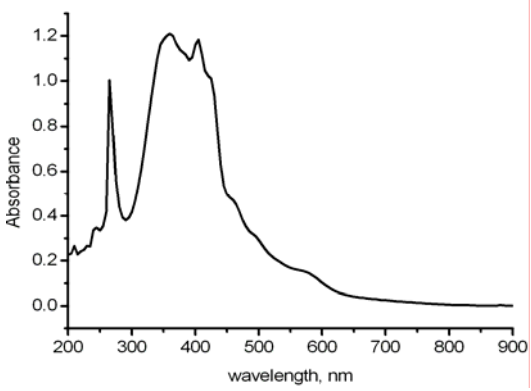

Figure 6.14: ***The UV-Vis spectrum of [Cu(hatp)Cl]***

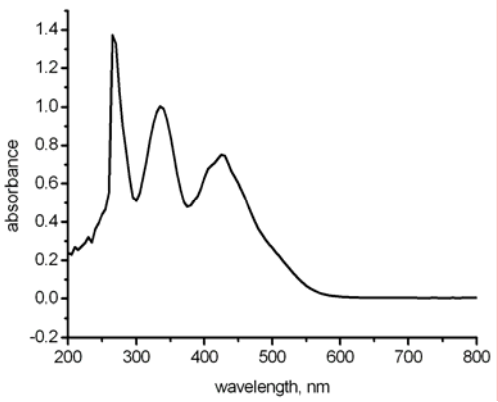

Figure 6.15: ***The UV-Vis spectrum of [Zn(hatp)(OAc)]***

6.3.5 Thermal analysis

Thermal stability of the btq and complexes of hatp was investigated using TG–DTG under nitrogen atmosphere with a heating rate of 10 ºC min^{-1} over a temperature range of 40–1000 ºC. The TG-DTG plots of btq and the complexes are given in figures 6.16-6.21.The compound btq exhibits a two stage decomposition which begins at 130 ºC. The weight loss observed for the cobalt(II) complex in the range 90-120 ºC indicates the presence of three lattice water molecules. The weight loss observed in the region 150-200 ºC for the manganese(II), cobalt(II) and nickel(II) complexes can be attributed to the loss of coordinated water molecules [35-37]. Table 6.6 presents the thermogravimetric analysis results below 220 ºC. The TG data suggest the presence of three coordinated water molecules in the cobalt(II) and nickel(II) complexes and two coordinated water molecules in the manganese(II) complex exhibit multi stage decomposition pattern. The data also show good agreement with the molecular formula of the complexes arrived from the analytical data.

Table 6.6: ***Thermogravimetric analysis data (below 220 ºC)***

Complex	Temperature range, ºC	% loss	Fragment lost	Nature of water lost
[Mn(hatp)(OAc)(H_2O)$_2$]	140-210	8.4	2 H_2O	Coordinated water
[Co(hatp)(H_2O)$_3$] H_2O	90-120	4.5	1 H_2O	Lattice water
	130-200	13.3	3 H_2O	Coordinated water
[Ni(hatp)(H_2O)$_3$]	140-220	13.7	3 H_2O	Coordinated water

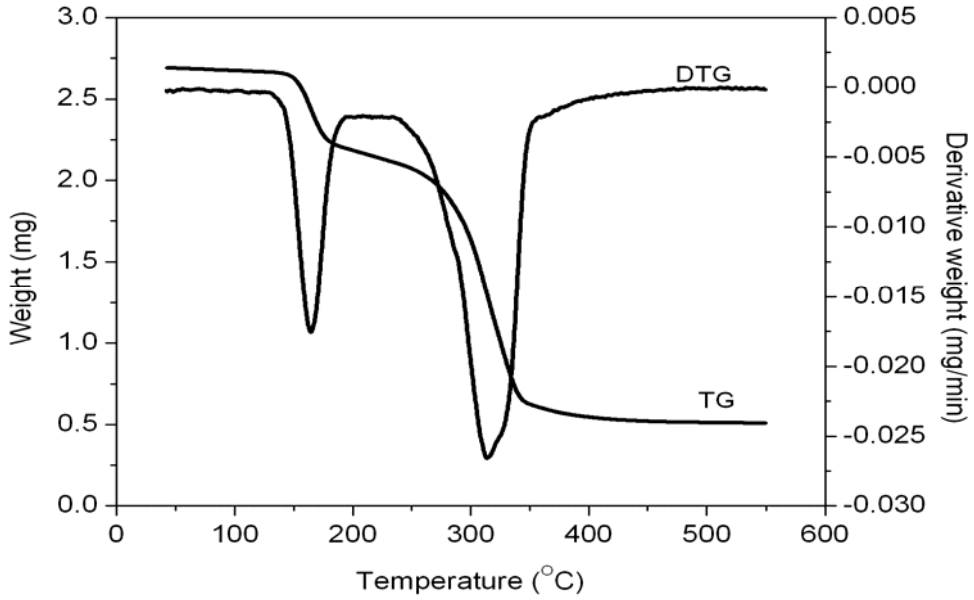

Figure 6.16: ***TG-DTG of btq***

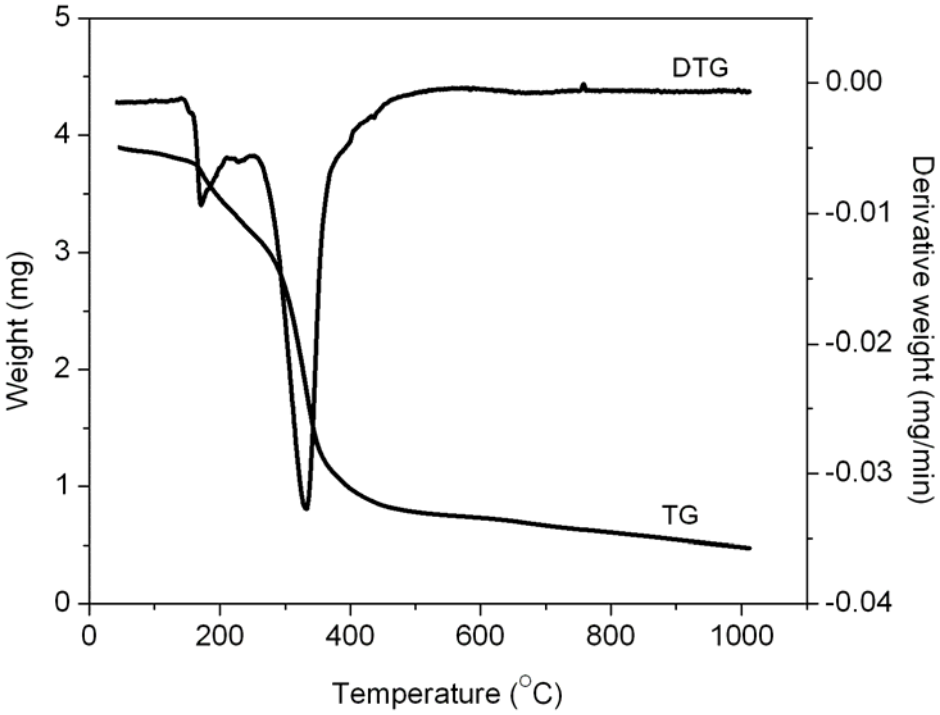

Figure 6.17: ***TG-DTG of [Mn(hatp)(OAc)(H$_2$O)$_2$]***

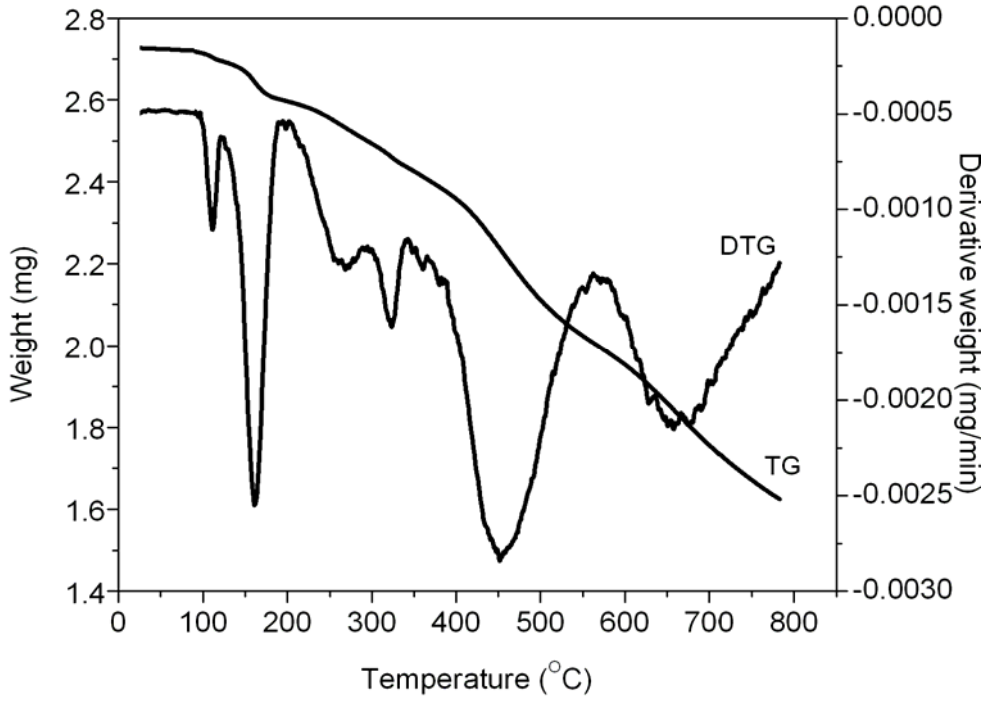

Figure 6.18: ***TG-DTG of [Co(hatp)(H$_2$O)$_3$]H$_2$O***

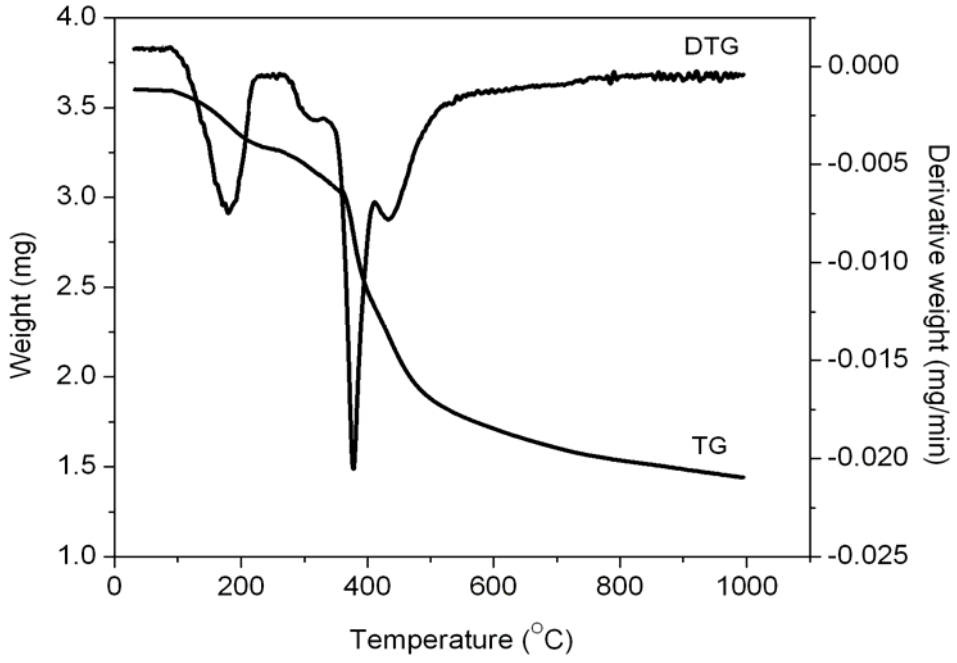

Figure 6.19: ***TG-DTG of [Ni(hatp)(H$_2$O)$_3$]***

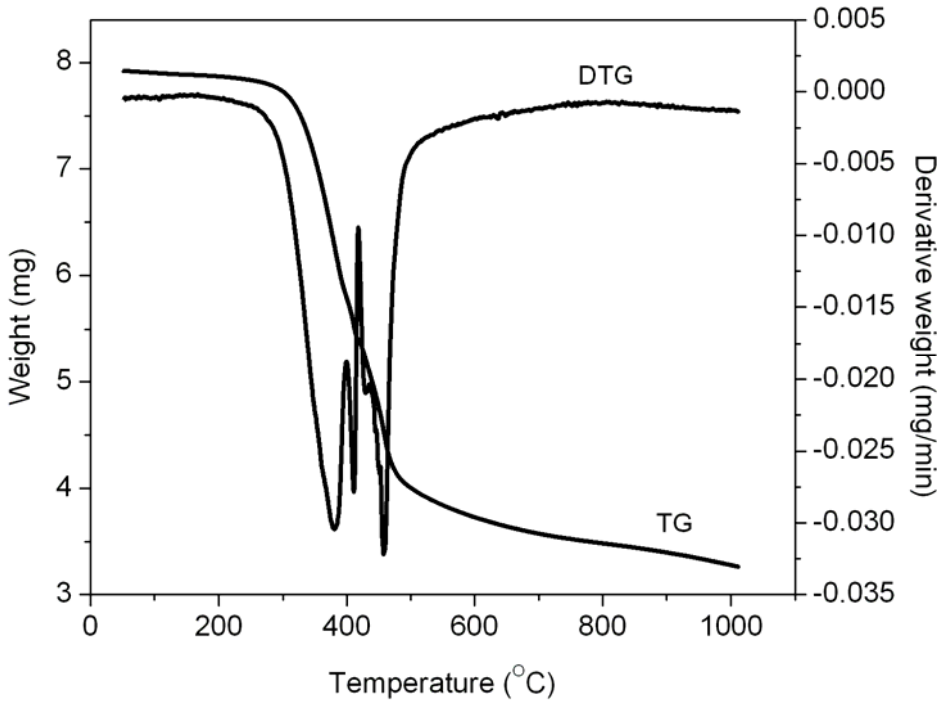

Figure 6.20: ***TG-DTG of [Cu(hatp)Cl]***

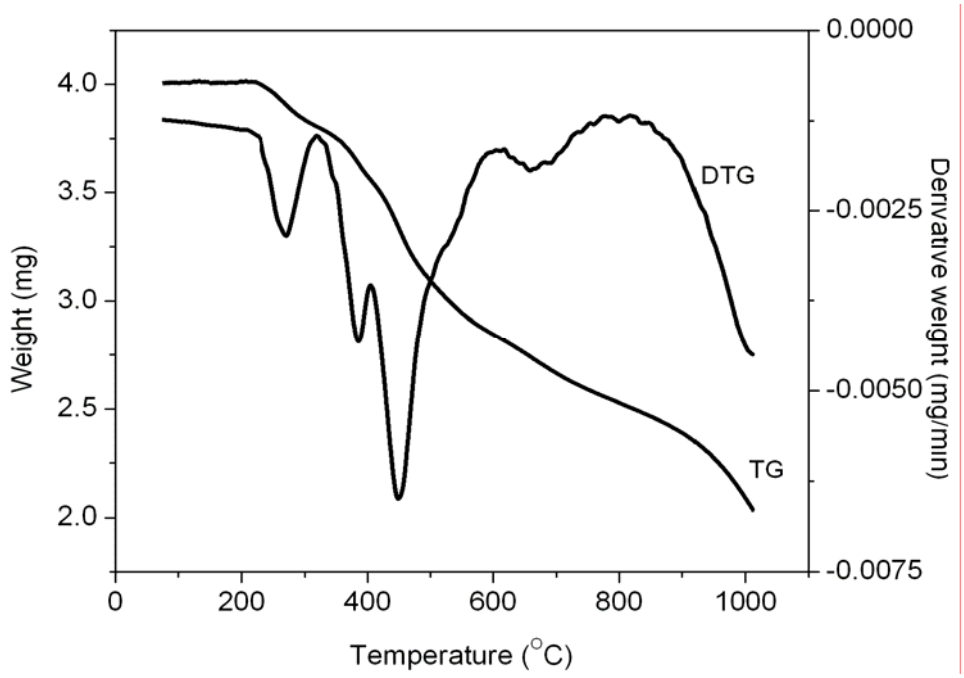

Figure 6.21: ***TG-DTG of [Zn(hatp)(OAc)]***

6.3.6 EPR spectra

The EPR spectra of the Cu(II) and Mn(II) complexes in the polycrystalline state at 298 K and in solution (DMSO) at 77 K were recorded in the X–band, using 100 kHz field modulation and the g tensors were calculated relative to the standard marker TCNE (g=2.003).

The solid state EPR spectrum of the Mn(II) complex is characterized by the broad isotropic spectrum with a g value of 1.98. The solution spectrum in DMSO at LNT gives six hyperfine lines which indicate the six allowed transitions. The low intensity spin forbidden transitions are observed in between the lines [38]. The spectrum gives a *g* value of 1.98 with an A value of 0.00851 cm^{-1} (Figure 6.22).

The copper(II) complex in polycrystalline state exhibits an isotropic spectrum with a g value of 1.97. This type of spectra gives no information on the electronic ground state of the Cu(II) ion present in the complexes [39]. EPR spectrum of the copper(II) complex in DMSO at liquid nitrogen temperature (figure 6.23) gives a $g_{\parallel}$ value of 2.20 and $g_{\perp}$ value of 2.08. The spectrum clearly reveals axial features ($g_{\parallel}>g_{\perp}>2.0023$), which suggests a B_{1g} ground state and a square planar geometry for the copper(II) complex [40, 41].

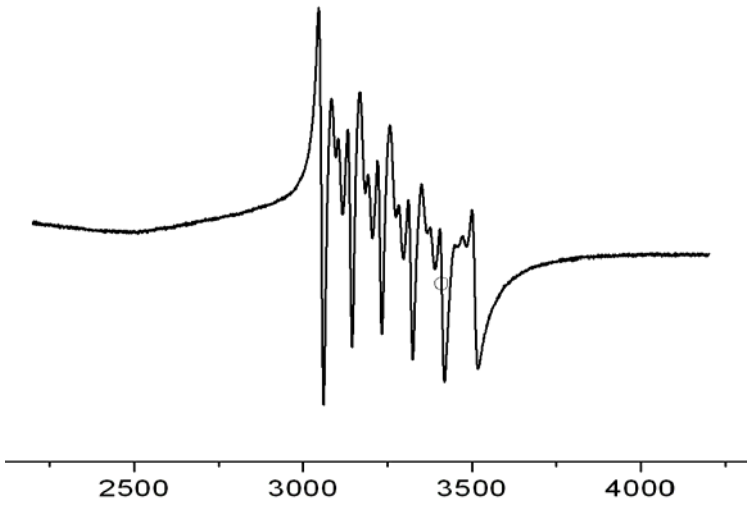

Figure 6.22: ***EPR spectrum of the Mn(II) complex in DMSO at LNT***

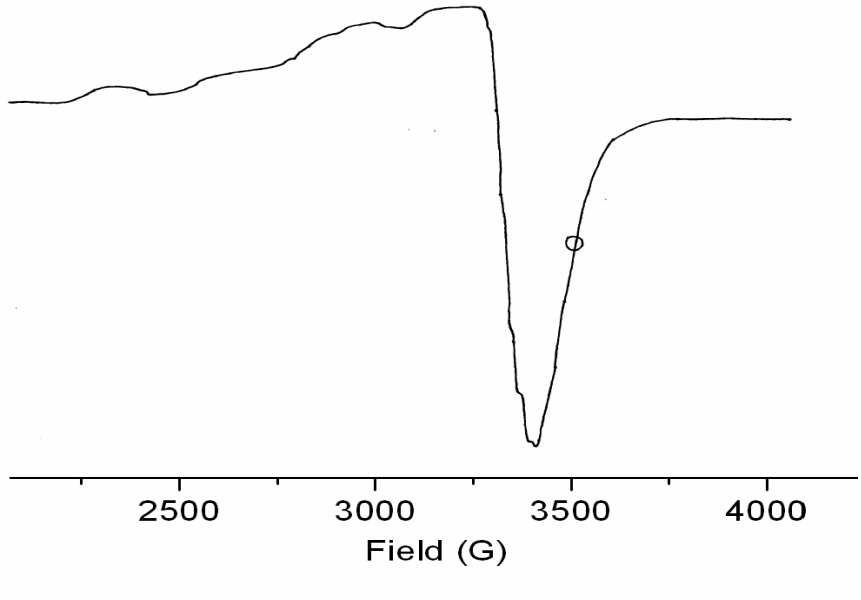

Figure 6.23: ***EPR spectrum of the copper(II) complex in DMSO at LNT***

6.4 CONCLUSIONS

A novel benzothiazolidine derivative, 3-(2,3-dihydro-1,3-benzothiazol-2-yl)quinoxalin-2(1*H*)-one, has been synthesized and characterized by elemental analysis, IR and NMR spectra. This compound (btq) gets rearranged to form tridentate ONS donor Schiff base, hatp, in the presence of metal ions. Like the other 3-hydroxy derivatives of quinoxalines, the compounds btq and hatp exhibit prototropic tautomerism. The Schiff base, hatp may get coordinated either in the keto form or in the enol form. All the complexes were characterized by physicochemical and spectroscopic techniques. These studies suggest that the copper(II) complex is square planar, zinc(II) complex is tetrahedral and the manganese(II), cobalt(II) and nickel(II) complexes are octahedral in geometry (figure 6.24).

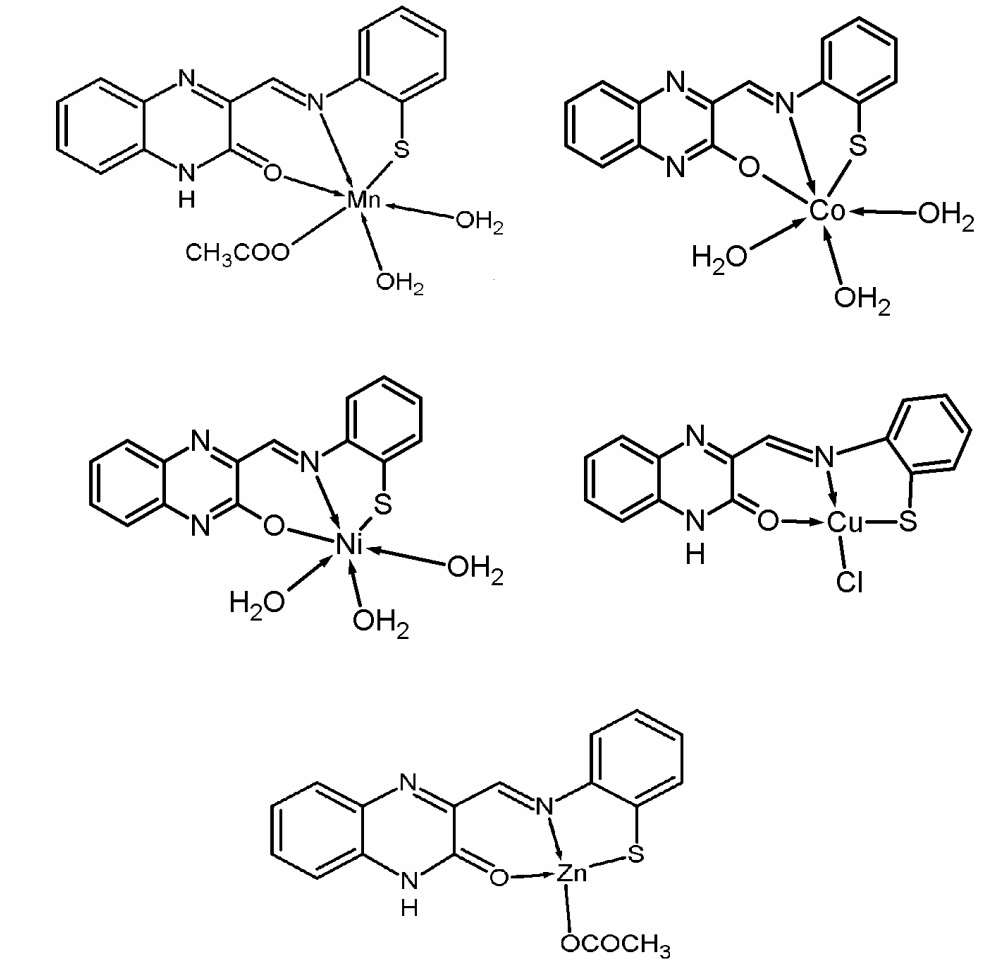

Figure 6.24: ***The proposed geometry of the complexes***

References

1. T. Daniel, T.D. Thangadurai, K. Natarajan, *Synth. React. Inorg. Met.-Org. Chem.* 31(4) (2001) 549.

2. R.C. Sharma, V.K.Varshney, *J. Inorg. Biochem.* 41 (1991) 299.

3. A.A. Soliman, W. Linert, *Monatshefte fuŕ Chemie* 138 (2007) 175.

4. J.R. Anacona, V.E. Marquez, *Transition Met. Chem*. 33 (2008) 579.

5. J.R. Anacona, V.E. Marquez, Y. Jimenez, *J. Coord. Chem.* 62 (2009) 1172.

6. E. Bouwman, R.K. Henderson, A.K. Powell, J. Reedijk, W.J.J. Smeets, A.L. Spek, N. Veldman, S. Wocadlo, *J. Chem. Soc*., *Dalton Trans*. (1998) 3495.

7. H. Damus, Q. Fernaxdo, H. Reiser, *Inorg chem.* 3 (1964) 928.

8. N.M. Shavaleev, R. Scopelliti, F. Gumy, J.-C.G. Bunzli, *Inorg. Chem.* 48 (2009) 6178.

9. M.K. Koley, S.C. Sivasubramanian, B. Varghese, P.T. Manoharan, A.P. Koley, *Inorg. Chim. Acta* 361 (2008) 1485.

10. A. Duatti, A. Marchi, R. Rossi, L. Magon, E. Deutsch, V. Bertolasi, F. Bellucci, *Inorg. Chem.* 27 (1988) 4208.

11. S.-H. Yoon, S. Seo, Y. Lee, S. Hwang, D.Y. Kim, *Med. Chem. Lett.* 8 (1998) 1909.

12. I.W. Boyd, J.T. Spence, *Inorg. Chem.* 21 (1982) 1602.

13. D. Shanker, R.K. Sharma, J. Sharma, A.K. Rai, Y.P. Singh, *Heteroat. Chem.* 18 (2007) 70.

14. W.J. Geary, *Coord. Chem. Rev*. 7 (1971) 81.

15. A.H.M. Elwahy, *Tetrahedron* 56 (2000) 897.

16. N. Raman, A. Kulandaisamy, K. Jeyasubramanian, *Synth. React. Inorg. Met.-Org. Chem.* 31(2001) 1249.

17 F.A.Cotton, G. Wilkinson, C.A. Murillo, M. Bochmann, *Advanced Inorganic Chemistry*, sixth ed., Wiley, New York (1999).

18 R. Janes, E.A. Moore, *Metal-ligand bonding*, Page 39, Royal Society of Chemistry, Cambridge, UK.

19 R.S. Drago, *Physical Methods in Inorganic Chemistry*, Rein Hold, New York, NY, USA, 1965.

20 M.R. Maurya, A. Kumar, A.R. Bhat, A. Azam, C. Bader, D. Rehder, *Inorg. Chem.* 45 (2006) 1260.

21 R. Gup, B. Kırkan, *Spectrochim. Acta A* 62 (2005) 1188.

22 V.A. Mamedov, A.A. Kalinin, N.M. Azancheev, Y.A. Levin, *Russ. J. Org. Chem.* 39 (2003) 125.

23 V.A. Mamedov, A.A. Kalinin, A.T. Gubaidullin, O.G. Isaikina, I.A. Litvinov, *Russ. J. Org. Chem.* 41 (2005) 599.

24 V.A. Mamedov, A.A. Kalinin, A.T. Gubaidullin, I.Z. Nurkhametova, I.A. Litvinov, Y.A. Levin, *Chem. Heterocycl. Comp.* 35 (1999) 1459.

25 K. Nakamoto, *Infrared and Raman Spectra of Inorganic and Coordination Compounds*, 4th ed., John Wiely and Sons, Inc, New York (1986).

26 E.B. Seena, N. Mathew, M. Kuriakose, M.R.P. Kurup, *Polyhedron* 27 (2008) 1455.

27 S. Mayadevi, K.K.M. Yusuff, *Synth. React. Inorg. Met.-Org. Chem.* 27(1997) 319.

28 S.M. Abdallah, G.G. Mohamed, M.A. Zayed, M.S. Abou El-Ela, *Spectrochimica Acta A*, 73 (2009) 833.

29 H.M. El-Tabl, F.A. El-Saied, M.I Ayad, *Synth. React. Inorg. Met.-Org. Chem.* 32 (2002) 1245.

30 Farona, M.F., Perry, D.C., Kuska, H.A., *Inorg. Chem.* 7 (1968) 2415.

31 M. Shebl , *Spectrochimica Acta A* 73 (2009) 313.

32 A.B.P. Lever, *Inorganic Electronic Spectroscopy*, 2nd Edn, Elsevier, Amsterdam (1984).

33 J.E. Huheey, *Inorganic Chemistry: Principles of Structure and Reactivity*, Harper and Row, NewYork, NY, USA (1980).

34 K.V. Sharma, V. Sharma, R.K. Dubey, U.N. Tripathi, *J. Coord. Chem.* 62 (2009) 493.

35 P.E. Aranha, J.M. Souza, S. Romera, L.A. Ramos, M.P. dos Santos, E.R. Dockal, E.T.G. Cavalheiro, *Thermochim. Acta* 453 (2007) 9.

36 N. Wasi, H.B. Singh, *Synth. React. Inorg. Met.-Org.Chem.* 18 (1988) 473.

37 H. M. Parekh, M. N. Patel, *Russ. J. Coord. Chem.* 32 (2006) 431.

38 M. Odehnal, *Czech. J. Phys.* 13 (1963) 566.

39 T.A. Reena**,** M.R.P. Kurup, *Spectrochim. Acta A* 76 (2010) 322.

40 R.N. Patel, V.L.N. Gundla, D.K. Patel, *Indian J. Chem. Sect. A* 47 (2008) 353.

41 S. Mayadevi, P.G. Prasad, K.K.M. Yusuff, *Synth. React. Inorg. Met.-Org. Chem.* 33 (2003) 481.